

The kinematics of stratified mixing through internal wavebreaking

By A. D. McEWAN†

CSIRO Division of Atmospheric Physics, P.O. Box 77, Mordialloc, Victoria 3195, Australia

(Received 24 April 1980 and in revised form 18 August 1982)

The evolution of an internal wavebreaking event in a continuous stable stratification is examined using schlieren colour imagery combined with streak photography. For standing but strongly interacting wavemodes forced to breaking, the Richardson number defined by local gradients of density and velocity is critically low only in the immediate vicinity of the breaking region where convective overturning also occurs. Breaking and vertical mixing results from the rapid development of three-dimensional interleaving density microstructure within a confined volume which persists and gravitates to modify weakly the surrounding density distribution. Continual mixing through internal motion is seen as a widespread repetition of such events.

Based on the observations, a general description of the process is proposed and applied in two types of simple kinematical model to provide an estimate of 'mixing efficiency', the ratio of potential energy gained through stratification weakening to kinetic energy expended in motions on the scales of the mixing event. These models do not rely on an assumed similarity between momentum and buoyancy transfer. They yield, for complete homogenization of small discrete volumes, an efficiency of $\frac{1}{4}$ in a linear stratification. Mixing across a density interface is predicted to have a lower efficiency, and lower efficiency is expected where homogenization is incomplete.

1. Introduction

In a stably stratified fluid, motions lose kinetic energy both by viscosity and by irreversible working against gravity to destroy the stratification. The partition of energy between these sinks is of fundamental importance in a variety of natural applications, since it determines the rate of vertical diffusion of matter and momentum in terms of energy input.

In the atmosphere and the ocean kinetic energy is transferred efficiently through a wide range of scales of motion, but appears to be dissipated mostly in discrete internal events of small scale through the continual reattainment of a state of dynamical instability (Woods 1980). It is possible that there is some generality in the transfer properties of such 'mixing events'. This is indeed tacitly assumed in the property-exchange arguments on which all theoretical estimates of vertical diffusion have been based. In particular, because often the kinetic energy is derived from vertical gradients of horizontal velocity, an analogy might be presumed to exist between processes of vertical transfer of buoyancy and momentum. If so, it is easily shown (Turner 1973) that the mixing efficiency η , defined as the ratio of the gain in

† Present address: CSIRO Division of Oceanography, P.O. Box 21, Cronulla, N.S.W., Australia.

potential energy of the system to kinetic energy lost as a result of a mixing event, is

$$\eta = \kappa_d Ri / \kappa_M, \quad (1)$$

where κ_d and κ_M are diffusivities of buoyancy and momentum respectively and Ri is the gradient Richardson number $N^2/(du/dz)^2$, where $N(z)$ is buoyancy frequency and du/dz is vertical gradient of horizontal velocity.

Since both momentum and buoyancy transfer are the result of the same event, the diffusivities might be presumed equal. Then, if, as postulated by Richardson (1920), all the kinetic energy lost goes to potential energy gained ($\eta = 1$), Ri for such events should be unity. Similarly, by assuming profile shape, constraints on the initial Ri and the growth of a shear layer following mixing can be determined (e.g. Turner 1973; Linden 1979) in terms of η .

Conversely, as discussed by Thompson (1980), if an event is discrete in space and time and has boundaries defined by some critical mean Richardson number Ri_c (arguably $\frac{1}{4}$) then η will have the same value.

This work presents a different conceptual approach to determine the mixing efficiency. It is based on the evidence of laboratory experiments revealing in quantifiable detail the evolution of internal mixing events. These experiments described in §2 employ internal wavebreaking as a means of providing well-controlled repeatable and observable behaviour.

In common with Browand & Winant's (1973) detailed visualizations of Kelvin-Helmholtz billow formation, the earliest stages of dissipative mixing are evidently a finescale filamentary interleaving of isopycnal surfaces.

Such events are evidently a transition to three-dimensionality and turbulence brought about by gravitational destabilization. They defy analytic description; but the observation that they involve at any moment only a small part of the total fluid volume and result in the irreversible destruction of potential energy gained from the larger-scale kinetic energy affords the basis for proposing some generalizations of the stratified mixing process. These are given in §3. From them emerges a new kinematical approach to the prediction of mixing efficiency, avoiding the conventional assumptions of similarity between buoyancy and momentum transfer. Some indeterminacy remains because the result depends on the manner and degree of mixing; and no account is taken of peripheral effects such as energy lost by wave radiation. Nevertheless some interesting results emerge. In particular it is found that, if a discrete volume in a linear stratification is overturned and subsequently homogenized, the mixing efficiency is one quarter, in accord with results reported in the companion paper (McEwan 1983). It is also shown that the efficiency rises with the quantity of mixed fluid produced through combination with its surroundings, and, when mixing occurs across a density step, the efficiency increases with step thickness. Incomplete mixing lowers the mixing efficiency.

The models are further discussed in §5, and compared with experimental estimates of mixing efficiency, reported in the companion paper.

2. Visualization of the kinematics of a wavebreaking event

Experiments were performed in a rectangular glass tank with a working section 12 cm wide and 50 cm long filled to a depth of 25 cm with an initially linear stratification of salt water with a buoyancy frequency $N = (g\rho^{-1}d\rho/dz)^{\frac{1}{2}}$ near mid-depth of 1.23 s^{-1} . A schlieren optical system incorporating two 30 cm mirrors aligned on

Colour	Vertical component of density gradient
Black	Unstable ($d\rho/dz > 0$)
Blue	0-0.6
Magenta	0.6-0.8
Red	0.8-1.2
Yellow	1.2-1.4
Green	1.4-2.0
Black	> 2.0 (double static stability)

TABLE 1. Schlieren colour code; density gradients are normalized by the static gradient near mid depth, $-1.57 \times 10^{-3} \text{ g cm}^{-4}$

the central lateral axis of the tank was arranged so that the image of the working section was formed on the focal plane of a motor-driven 35 mm still camera. The light source was a 35 mm colour transparency with a diffusing screen set into a conventional slide projector without its front lens. The image of the slide was formed on a 2 mm wide horizontal slit immediately in front of the camera lens. The slide itself was graded in horizontal bands of blue, red and green, and the system was arranged so that vertical components of density gradient were coded on the image as in table 1.

In addition to the schlieren illumination, the working section was lit in a 1 cm wide vertical band by light from a second projector, and was also scanned vertically in the centre of the same band by the light from a laser, reflected from a mirror which was oscillated at modulated frequency by a magnetic driving unit. With numerous neutrally buoyant polystyrene beads of 1 mm diameter in suspension in the fluid, this afforded the means of indicating both velocity and direction of fluid in relation to the schlieren density-gradient visualization. To provide a streak photograph of particle movement while freezing the schlieren image, a chopper disk was placed in front of the schlieren projector. The camera was actuated magnetically in synchronization with the disk.

The purpose behind these efforts was primarily to provide a direct and extensive indication of instantaneous gradient Richardson number. For the observations presented here the streak exposure was 0.5 s; thus if δl is the difference in length between adjacent streaks and δn their normal spacing the shear magnitude is about $1.63 N \delta l / \delta n$.

A standing, primary-mode internal wave (vertical and horizontal wavelengths each twice the tank dimensions) was forced continuously at resonance by a sealed paddle forming one end of the working section. Such a wave becomes susceptible at small amplitude to resonantly interactive instability (McEwan 1971) and can be brought gradually to a condition of isolated 'breaking', evidently through the nonlinear interaction between the generated parasitic modes, in an orderly and repeatable fashion.

The procedure was to bring the fluid to a state of incipient breaking and then start photographing at five frames every four seconds over 30 s of the evolution of the first breaking event.

Figures 1(a-c) (plates 1-3) show important stages in the evolutionary process. Reference is made relative to the coordinate grid at ± 10 cm on each side of the working-section axis, and ± 5 cm above and below. The uppermost horizontal line is the free surface.

From table 1, the region of black bordered by blue is statically unstable, while blue

represents density gradients in the range 0–0.6 times the static density gradient ($-0.0016 \text{ g cm}^{-4}$). Figure 1(a), taken 2.4 s after the first appearance of static instability, shows a region of positive density gradient at (5, 0) in (x, y) (centimetre coordinates) bounded to the right below by a region of strong gradient (black bounded by green). The motion is predominantly two-dimensional, although small patches of fine-scale distortion (evidently three-dimensional by the occasional ‘crossing’ of particle paths) have appeared at (5, 4), (14, 3), (–7, –2) and (3, –2). Throughout the field the shear is low, except for a particle pair within the unstable region indicating a shear of 1.9 N, and another zone of similar strength at (–1, –3). Such shears seem to be extremely localized, and both lie within regions of weakened (or non-existent) stability. The Richardson number based on vertical density gradient is correspondingly low in these locations, but well above unity elsewhere.

In figure 1(b), 1.6 s later, static stability (averaged along the light path) has been restored through most of the region of interest at (5, 0), though lessened below static levels, but the field is now finely convoluted and the motion is three-dimensional, as evidenced by the crossing of particle streaks. Shear is much reduced. Unstable regions are appearing elsewhere in the field.

Figure 1(c), 7.2 s or roughly one half-period of the background wave later than 1(b), shows the density structure to have become much finer in scale and closer in mean gradient to the unperturbed level. It has also extended horizontally and has evidently enlarged in volume. Within the region shears are substantially reduced, and there is no sign that the density gradients bounding the mixed region have been sharpened.

Elsewhere in the fluid there have occurred other mixing events which have produced some fine-structure, but it is noted that the whole fluid has acquired a streaky texture indicative of layering structure of very fine scale, 1 mm or even less. Since the momentum diffusion timescale for such structure is very short, spontaneous generation by some unidentified dynamical process seems unlikely, but it is a ubiquitous phenomenon requiring very little visible breaking activity for its first appearance.

Several similar experiments were conducted, all yielding the same principal results, which can be summarized as follows.

(i) The motion remains laminar and two-dimensional until localized states of static instability are closely approached or exceeded.

(ii) Three-dimensional density microstructure characteristic of breaking appears abruptly in the locations of weakest static stability, and persists with a progressive refinement of scale for a period long compared with the momentum diffusion timescale.

(iii) The gradient Richardson number is lowered by loss of static stability and enhancement of shear in the immediate vicinity of subsequent mixing, but is not small elsewhere and therefore does not appear to be important in defining the onset of breaking of the kind reported here.

(iv) In the breaking regions, shear deformation on the scale of the background waves is low and the mean gradient of density is stable. There is no consistent evidence of sharpened density gradients at the boundaries of these regions.

(v) Very fine layering density microstructure becomes well distributed through the fluid, even beyond regions where breaking has occurred, with a rapidity that is hard to explain.

3. A qualitative general description of the dynamics of stratified mixing

From the present observations and a scrutiny of Browand & Winant's (1973) and other experimental studies, there emerge some identifiable features common to internal mixing events in stratified fluids at low Reynolds numbers, as follows.

(a) All significant vertical diffusion results from the creation of fine-scale three-dimensional interleaving of material surfaces. Molecular diffusion then proceeds through these surfaces across property gradients greatly enhanced over static equilibrium values.

(b) Such interleavings are confined to discrete regions which at a given time are normally a small part of the total fluid volume.

(c) The interleavings are the result of the rapid development of instabilities resulting from the attainment of some dynamical condition in the large-scale motion field within the same region. This condition is evidently 'convective instability' in which isopycnals are rotated beyond the vertical.

(d) The principal loss of energy from the large scales is due to the release of gravitational potential energy into the interleaving structures. This is not reversible as it would be for the larger scales because momentum exchange timescales in the interleaving structures are short, although property diffusion timescales may be long.

(e) For the same reason velocity gradients in interleaving regions are weak and the direct loss of kinetic energy from large scales is comparatively insignificant. Conversion of kinetic energy into wave potential energy always precedes final dissipation.

(f) A proportion of the large-scale kinetic energy is recovered by the gravitation of the fluid that has combined diffusively in the interleaving regions. This combination is not necessarily complete and depends on the kinematics of the interleaving process. Unless mixing in a single event is intense and occupies a significant proportion of the horizontal area at the level of its occurrence, discontinuities in density will not be produced.

(g) In steadily energized motion, mixing is the result of a continual recurrence of discrete destabilization events. These are frequently the result of internal waves radiated from previous events, but they are more or less independent of one another so far as their effect upon the stratification is concerned.

These elements are illustrated in figure 2. In figure 2(a) fluid between isopycnals $\rho = \rho_e$ and ρ_{-e} is convectionally destabilized within the material envelope e . If the stratification is weak, events are symmetrical on average about the central isopycnal ρ_0 .

In figure 2(b) fine-scale interleaving structure has started to develop within e . A quarter buoyancy period later (figure 2c) static stability is restored in the external field and on average within e , but the interleavings persist. Much later (figure 2d) the fluid within e has settled to its equilibrium level. In so doing the outer levels are depleted and gradients are strengthened, while near to the central level of the event mixed fluid has accumulated and the net gradients are weakened. The external isopycnals remain unaffected. A notional (and exaggerated) modification to a linear density profile is shown.

4. Particle-exchange models

Consider two fluid particles each with volume V at static levels z_0 and z_1 and densities ρ_0 and ρ_1 respectively, in an arbitrary stratification $\rho(z)$.

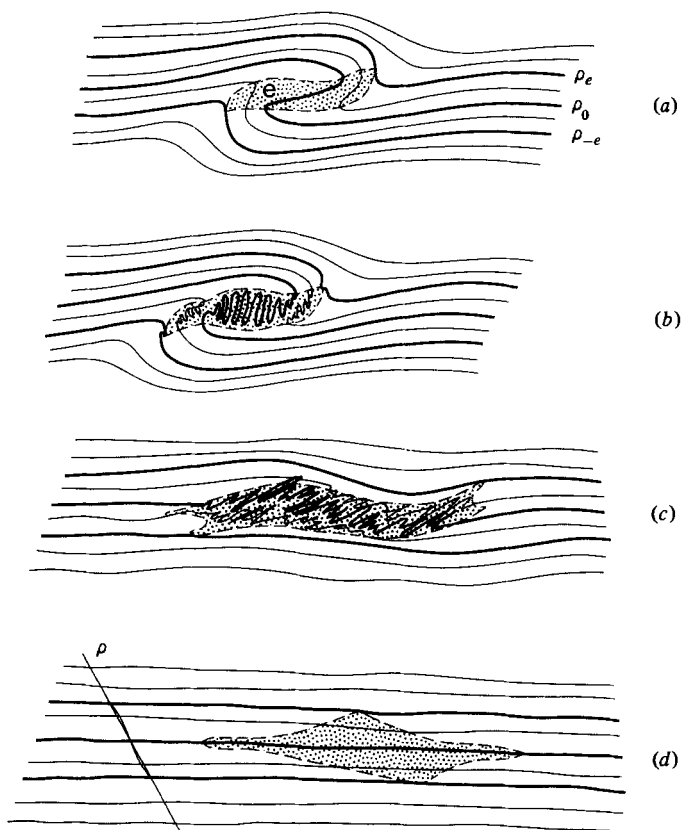


FIGURE 2. Idealization of a mixing event in a continuous stratification. (a) Overturning. (b) Development of interleaving microstructure. (c) Static stability is restored but microstructure is preserved. (d) Gravitation to an equilibrium has changed the surrounding density profile between extremum isopycnals. The distortion of the profile is exaggerated for clarity. The intermediate isopycnals (fourth and sixth from the top) are displaced upwards and downwards respectively from their original positions, representing a gain in stratification potential energy.

The horizontal area density of particle exchange events is $1/S$ and it is assumed that $V/S \ll z_1 - z_0$.

If the particles are exchanged as shown in figure 3(a), the work done on the whole fluid system is

$$E = gV(\rho_0 - \rho_1)(z_1 - z_0), \quad (2)$$

and in the case of a linear density profile $\rho'_0 = -(\rho_0 - \rho_1)/(z_1 - z_0)$

$$E = -g\rho'_0 V(z_1 - z_0)^2. \quad (2a)$$

The essence of this model is that E is gained from the disturbance field without dissipation. All losses result from the subsequent gravitation and mixing of the particles *without returning kinetic energy to the disturbance field*.

Clearly if the particles return without mixing with their surroundings the system gains no potential energy; hence the mixing efficiency is zero. However, if the particles are small enough or sufficiently deformed, molecular diffusion will ensure that they exchange their properties with their surrounds during the return. With a diffusion coefficient κ_s and a minimum natural timescale characterized by inverse buoyancy

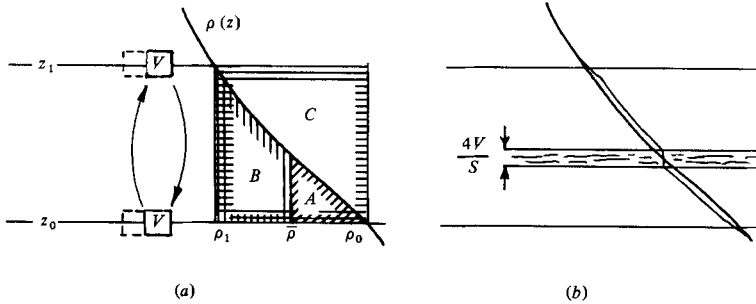


FIGURE 3. Particle-exchange models. (a) Particles at levels ρ_0 and ρ_1 are exchanged without modification of the surrounding profile $\rho(z)$. Diagonal hatching: area A . Vertical hatching: area B . Horizontal hatching: area C . (b) Redistribution of density following combination at new levels and gravitation to mixture density $\bar{\rho}$ level.

frequency $N^{-1} = [\rho_0(z_1 - z_0)/g(\rho_1 - \rho_0)]^{\frac{1}{2}}$ the lengthscale over which density is diffused would be of order

$$\delta_s = (\kappa_s/N)^{\frac{1}{2}}.$$

Similarly the lengthscale for diffusion of momentum in the same period is

$$\delta = (\nu/N)^{\frac{1}{2}},$$

below which scale viscosity would inhibit buoyant disengagement. This then defines the lengthscale of conventionally generated microstructure which is preserved after stability is restored following overturn. Its magnitude is of order 1 mm in the present experiments, and, providing the Prandtl number ν/κ_s is greater than unity, $\delta > \delta_s$. In the companion paper it is argued that gravitational flattening extends the untangling timescale such that even for high Prandtl numbers buoyancy diffusion will be complete providing δ is very much less than the vertical scale of the mixing region, as observed here. Also, for the present calculation, since properties are exchanged by diffusion proceeding more or less symmetrically it is reasonable to assume that the particle and its surroundings combine in equal proportion. The calculation can be extended easily to unequal proportion but such detail is not justified.

The mixing efficiency then becomes dependent on the manner in which the particle spreads during mixing, as the following fundamental examples will show.

4.1. *Particles combine with their new surroundings without prior gravitation*

The ρ_0 particle combines in equal proportion with its ρ_1 surroundings and vice versa, thus producing a volume $4V$ of fluid of intermediate density $\bar{\rho} = \frac{1}{2}(\rho_1 + \rho_0)$. This then gravitates to level $\bar{z} = z(\bar{\rho})$ and spreads horizontally at that level. After equilibration, levels z_0 and z_1 have each been depleted by volume $2V$ and level \bar{z} has been supplemented by $4V$. The result is a redistribution of density over S as shown in figure 3(b). The layer \bar{z} to z_0 has lost $2V/S$ in elevation and the layer \bar{z} to z_1 has gained $2V/S$. Beyond z_1 and z_0 the stratification is unaffected.

Potential-energy gain P is expressed by the change in the net potential energy of the system between levels z_0 and z_1 , i.e.

$$P = gS \int_{z_0}^{z_1} (\rho_1 - \rho_0) z dz, \quad (3a)$$

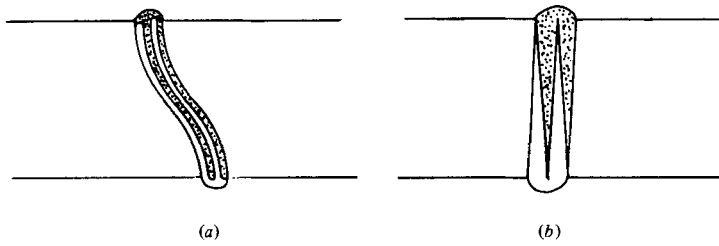


FIGURE 4. Particle interleaving. (a) Interleaving so that particles combine in equal proportion throughout. Profile changes are one-half of those of figure 3(b). (b) Wedge interleaving. Fluid combines horizontally in triangular proportion, and modifies gradients between ρ_1 and ρ_0 .

where subscripts f and i refer to final and initial profiles. From inspection of figure 3(b) $\rho_f(z) = \rho_i(z - j2V/S)$, where $j(z_1 > z > \bar{z}) = 1$ and $j(\bar{z} > z > z_0) = -1$. Thus to first approximation $\rho_f - \rho_i = 2\rho'jV/S$. Substituting in (3) and with (2), the mixing efficiency is then

$$\eta_a = \frac{P}{E} = \frac{2 \left(\int_{\rho_1}^{\bar{\rho}} z(\rho) d\rho - \int_{\bar{\rho}}^{\rho_0} z(\rho) d\rho \right)}{(\rho_0 - \rho_1)(z_0 - z_1)}, \quad (4)$$

where the variable of integration has been changed from z to ρ for convenience. In terms of the areas delineated in figure 3(a)

$$\eta_a = \frac{2(B-A)}{C}. \quad (4a)$$

Of particular interest is the case of a linear pycnocline of thickness δ separating fluids of density ρ_0 and ρ_1 for which

$$\eta_a = \delta/2(z_1 - z_0).$$

Thus if the stratification is linear over the vertical extent of the mixing, $\delta \geq z_1 - z_0$, then $\eta_a = \frac{1}{2}$. Note that η_a is independent of S .

4.2. Particles extend throughout the mixing depth and combine together

For the reasons outlined earlier, irreversible mixing relies on considerable strain deformation, which observation suggests is filamental and confined in volume. A more realistic representation of this than in §4.1 is to suppose that the particles interleave as in figure 4(a). If the interleaving is so fine that the mixture is homogeneous and of intermediate density $\frac{1}{2}(\rho_1 + \rho_0)$, but involves no external fluid, the volume produced is $2V$, which augments mid-level \bar{z} after gravitation, and levels z_0 and z_1 are each depleted by V . The only difference from the case in §4.1 is that quantities are halved, and correspondingly

$$\eta_b = \frac{B-A}{C}. \quad (4b)$$

So for a linear pycnocline as before, $\eta_b = \delta/4(z_1 - z_0)$ or for a linear profile $\eta_b = \frac{1}{4}$.

4.3. Finite volumes in a linear stratification

It is worth noting that in a linear stratification, finite volumes of any shape will combine in the same manner as in the case in §4.2, provided that the mixture is

homogenized completely. Thus if homogenization results from the collapse of a fully overturned discrete fluid volume the mixing efficiency of such an event is one quarter.

4.4. Particles combine to produce an inhomogeneous mixture

If mixing is incomplete, mixed fluid becomes distributed between z_0 and z_1 . The effect is illustrated by a simple example in which triangular wedges interleave as in figure 4(b), and then combine by lateral diffusion. Levels z_0 and z_1 are each depleted by V and intermediate levels are supplemented by $2V(\rho_1 - \rho_0)^{-1}$ per unit density change. Therefore each isopycnal level ρ is elevated by

$$q(\rho) = \frac{1}{S} \int_{\rho_0}^{\rho} \frac{2V}{\rho_1 - \rho_0} d\rho - \frac{V}{S} = \frac{V}{S} (2\rho - \rho_1 - \rho_0).$$

Integrating the potential energy gain between z_0 and z_1 and combining with (2) the resultant mixing efficiency is

$$\eta_c = \frac{\int_{z_0}^{z_1} \rho(2\rho - \rho_0 - \rho_1) dz}{(z_1 - z_0)(\rho_1 - \rho_0)^2}. \quad (4c)$$

So $\eta_c = \frac{1}{6}$ for a linear stratification, or $\delta/6(z_1 - z_0)$ for a linear pycnocline.

From each of (4a)–(4c) and reference to figure 3(a) it can be seen that the efficiency decreases with $\delta/(z_1 - z_0)$, because the final potential energy gained by the system is determined only by the thickening of the pycnocline, while from (2a) the energy input is scaled by the square of displacement distance $z_1 - z_0$.

5. Discussion

The approach presented here departs in two important ways from previous idealizations of stratified mixing. Firstly the events are assumed to be small in volume and discrete, so that the vertical transfer of properties is not characterized by the gradient of mean properties and the ‘mixing length’ over which these are transported, but by the manner in which fluid becomes distributed and combines within the discrete volume. Secondly, kinetic energy is not lost directly by momentum exchange, but by conversion to potential energy which is released in dissipative scales.

The pathway for the kinetic energy is assumed to be directly through conversion to potential energy, then to diffusive-scale kinetic energy, and directly to viscosity. This accords with the present observations, but perhaps should be regarded with caution with respect to very energetic or large-scale overturns with high Reynolds numbers. The justification for this assumption is that kinetic energy not lost by this pathway becomes available again for further mixing by conversion back into scales larger than the diffusive scales. Thus the kinematic details of these larger scales are presumed unimportant. In general the validity hinges upon the separation between buoyancy and viscous subscales, and is discussed further in the companion paper (McEwan 1983).

In putting numbers on the mixing efficiency, indeterminacy remains because the calculation includes only the losses from the large-scale motion into fine-scale potential energy; incidental kinetic-energy loss and work done in straining the mixed volume are neglected. Furthermore, the final potential energy gained by the stratification depends on the details of mixing, which remain unknown. The values obtained for the examples given are therefore only representative estimates. However,

they rest on assumptions no less justifiable than previous theories, and some useful results emerge.

In particular, the efficiency is predicted to be one quarter when homogenization is complete within discrete volumes in a linear stratification. This agrees with the value often assumed in diffusion calculations, and is also in very good accord with the experimental measurements of McEwan (1983), wherein internal waves were forced continuously to saturated breaking in an initially linear stratification. Efficiencies of between 0.15 and 0.36 were obtained, with an average of 0.26 and a standard deviation of 0.06. The results were not significantly correlated with estimated minima in gradient Richardson number, nor with net internal dissipation rate. These findings lend some support to the proposition on which the present models are based that there are general properties of internal mixing in stratified fluids which depend only on the kinematics of discrete events. The rate of energy supply determines the frequency of mixing events but not their efficiency of conversion into net stratification potential energy.

Another interesting result from the particle-exchange model is that mixing efficiency declines with interfacial thickness. In practical terms mixing events that are much deeper than the interface at which they occur might be expected to yield a lower mixing efficiency. Almost all of the experiments reviewed by Linden (1979) concern interfacial mixing, and these give efficiencies (flux Richardson number) ranging downwards from 0.2. Close comparison with the present observations and theory is not warranted both because some experiments employed mechanical mixing and because allowance could not be made for viscous and turbulent dissipation incidental to the mixing process. Each of these factors would tend to lower the estimate, and produce the form of dependency upon Richardson number noted by Linden, namely an approach to zero efficiency as stratification vanishes and a gradual descent as Richardson number rises from about $\frac{1}{4}$.

A third result is that if mixing is not complete the efficiency will be lowered because the mixed volume will have gained less than the maximum possible potential energy.

Finally, it is worth noting that the generalizations proposed here and the models based on them, turn out to be not particularly appropriate to intense Kelvin–Helmholtz billowing, because in this kind of mixing the volume of the billows is not a small proportion of the total volume through the mixing depth. Furthermore, as analysed by Corcos & Sherman (1976) and Koop & Browand (1979), the process of kinetic-energy loss from the mean shear is largely by the concentration and diffusion of vorticity in the billow cores, and the final disintegration of these cores. Although some potential energy would be gained within the cores, much of the energy loss must occur by vorticity diffusion at the boundary of each core, and the cores are well-mixed gyres coupled to the external field mainly by viscosity.

It can be asserted that, because of this direct kinetic energy loss through viscosity, the mixing efficiency of Kelvin–Helmholtz billows could be less than the present models would predict.

The assistance of I. Helmond and G. Scott in conducting the experiments is gratefully acknowledged.

REFERENCES

- BROWAND, F. K. & WINANT, C. D. 1973 Laboratory observations of shear-layer instability in stratified fluid. *Boundary-Layer Met.* **5**, 67–77.

- CORCOS, G. M. & SHERMAN, F. S. 1976 Vorticity concentration and the dynamics of unstable free shear layers. *J. Fluid Mech.* **73**, 241–264.
- KOOP, C. G. & BROWAND, F. K. 1979 Instability and turbulence in a stratified fluid with shear. *J. Fluid Mech.* **93**, 135–159.
- LINDEN, P. F. 1979 Mixing in stratified fluids. *Geophys. Astrophys. Fluid Dyn.* **13**, 3–24.
- MC EWAN, A. D. 1971 Degeneration of resonantly excited internal gravity waves. *J. Fluid Mech.* **50**, 431–448.
- MC EWAN, A. D. 1983 Internal mixing in stratified fluids. *J. Fluid Mech.* **128**, 59–80.
- RICHARDSON, L. F. 1920 The supply of energy from and to atmospheric eddies. *Proc. R. Soc. Lond. A* **97**, 354–373.
- THOMPSON, R. O. R. Y. 1980 Efficiency of conversion of kinetic energy to potential energy by a breaking internal wave. *J. Geophys. Res.* **85**, 6631–6635.
- TURNER, J. S. 1973 *Buoyancy Effects in Fluids*. Cambridge University Press.
- WOODS, J. D. 1980 Do waves limit turbulent diffusion in the ocean? *Nature* **288**, 219–224.

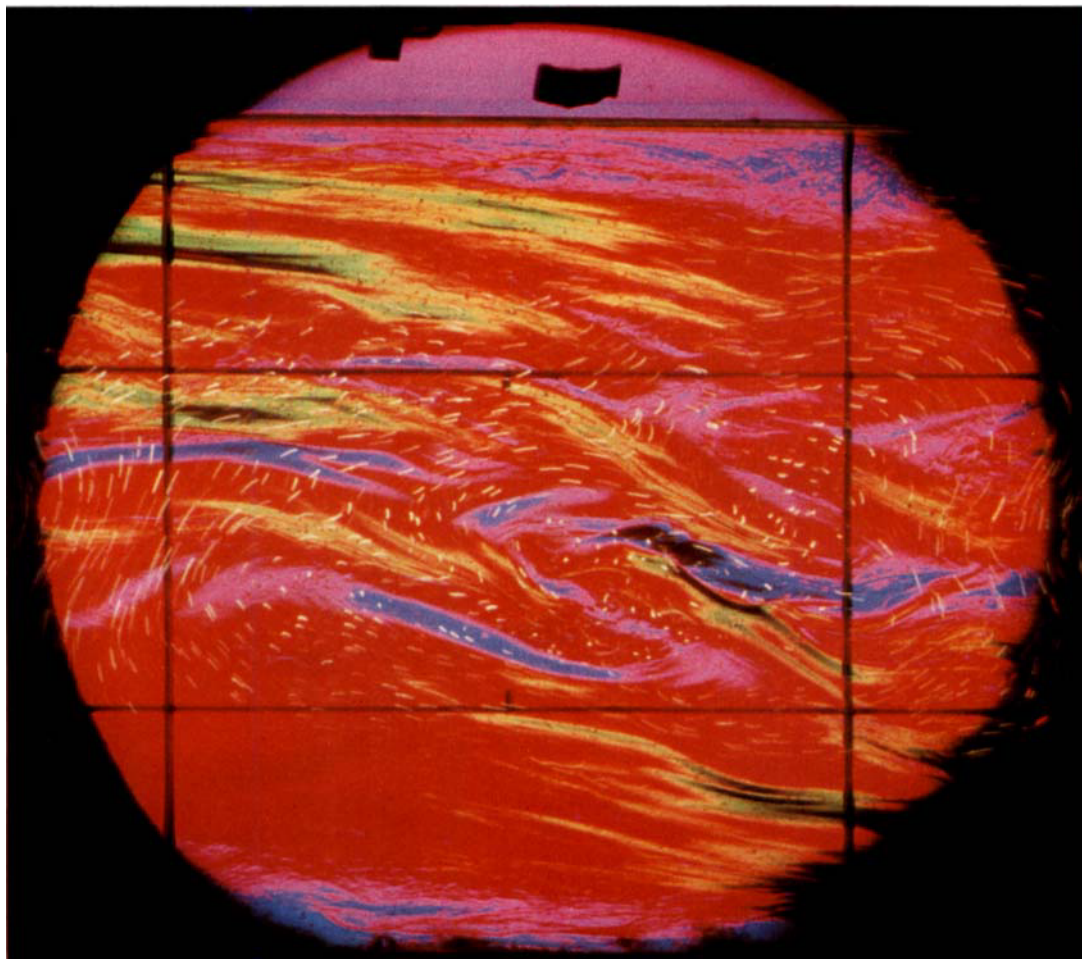


FIGURE 1 (*a*). For caption see plate 3.

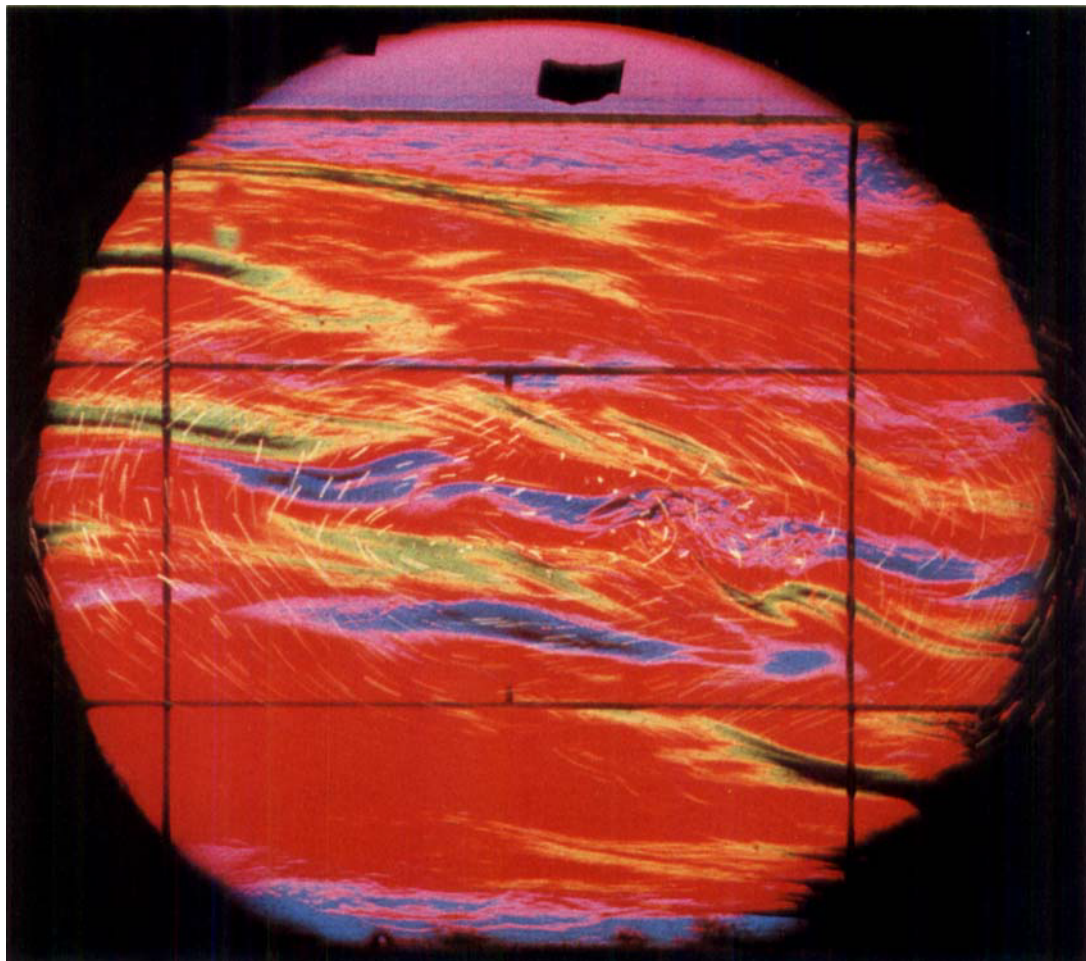


FIGURE 1 (b). For caption see plate 3.

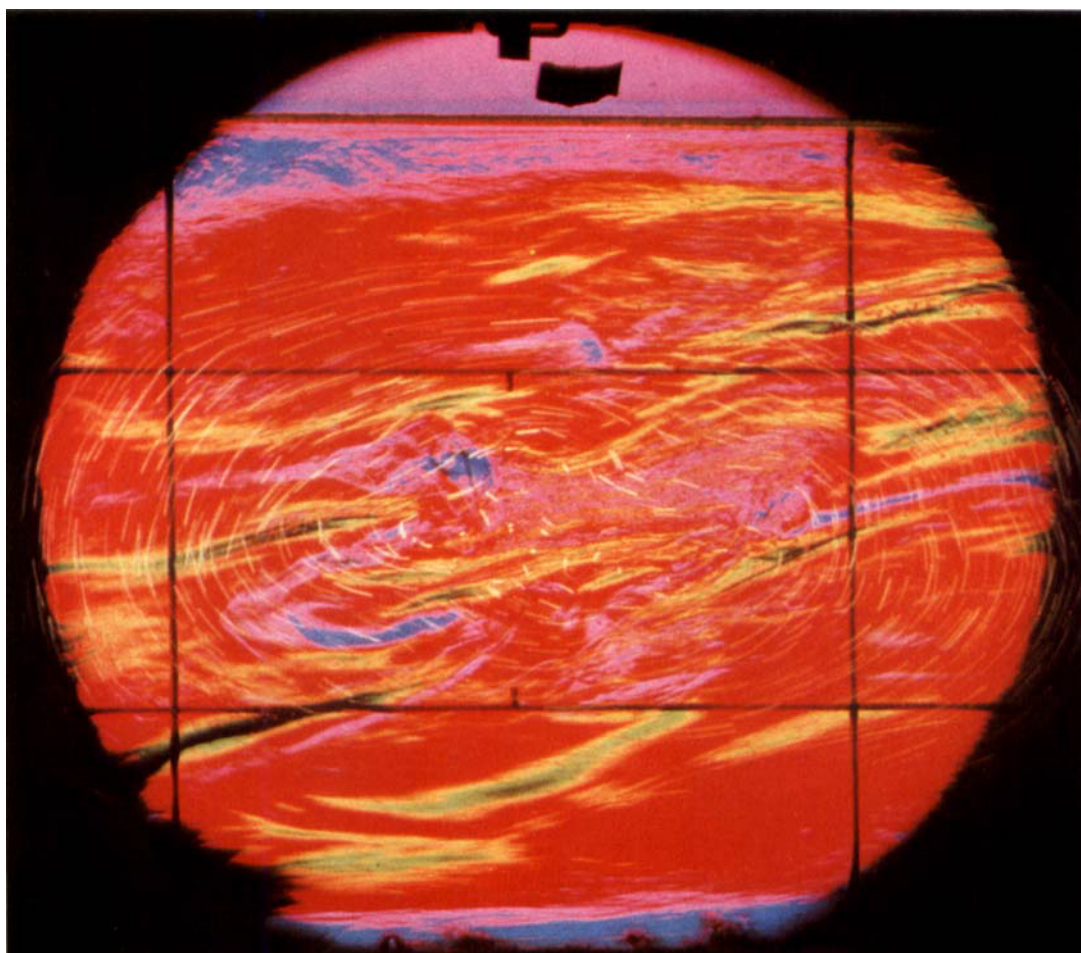


FIGURE 1. Schlieren visualization of stages of a breaking event induced by internal wave action in a continuously stratified fluid. The image is colour-coded by vertical density gradient according to the scale given in table 1. In addition particle streaks revealed by half-second exposure are superimposed. Background wave period is 14 s. Further details are given in the text. (a) 2.4 s after static instability is first observed. (b) 1.6 s later than (a). (c) 7.2 s later than (b).